

---

---

## Computer fluids dynamics a horizontal axis wind turbine blade: the aerodynamics of airfoils

\*Nabil Ali Alfeetori

\*Abdulhafiz Younis Mokhetar

---

---

### Abstract

This article addressed 2D design and simulation. also has been shown the best performance for tow airfoils design To generate the data from the fluid flow situations, it may employ the two programs solidworks and FLUENT. Choose the NACA airfoil models NACA1410 and NACA24112 for this study. NACA 1410 was chosen because it has a higher lift coefficient than NACA 24112. In this study, two-dimensional airfoil NACA 1410 and NACA 24112 CFD models are provided using ANSYS-FLUENT software to simulate computational flow through an airfoil at various angles of attack ( $0^\circ$ ,  $7^\circ$ ,  $14^\circ$ ,  $30^\circ$ , and  $50^\circ$ ). Using this design Using the conventional wall function's k-epsilon turbulent viscosity near the wall and the wind's 10 m/s speed Here, the study of wind turbine blades takes into account the NACA 1410 airfoil profile. solidworks and CFD are used to develop the airfoil's geometry.

**Key words:** CFD simulation, airfoil, angle of attack.

### 1. Introduction

The cross section of a body positioned in an airstream in order to generate a useful aerodynamic force as effectively as feasible is referred to as an airfoil. (H. Abbott, 2010) The creation of an airfoil model like the NACA 1410 or NACA 24112 required an understanding of aerodynamic qualities. The mesh generation with boundary criteria was clustered and picked using the solidworks to construct it. (O. L. Hansen, 2008) A number of earlier studies, including those by Badran and Bruun. (Basuno & Abdullah 2001) Air traveling through a streamlined

\*Staff member faculty of engineering university of Triploi – Libya

\*\*Staff member faculty of engineering university of Triploi – Libya

body exhibits a physical flow phenomena that demonstrates the viscous effect is only present in the flow zone close to the surface of the body. (O. Badran and H. Bruun) The ability to forecast boundary layer separation on the NACA 1410 airfoil at various positions of angle of attack is investigated using two-equation turbulence models. The k-epsilon two equation model. Seetharam and Wentz, (D. Adair, 1987) have looked at the aerodynamic characteristics of the NACA 1410 airfoil section. This is because the performance of aerodynamic at the upper surface of the airfoil would be restricted by turbulent boundary layer separation. In addition to Woodcock, Badran, Kayiem, and Nakayama, ( D. Coles, A.Wadcock, 1979) collected the most precise data in the separated flow zone over airfoils. This study uses computational fluid dynamics (CFD) to analyze the aerodynamics of airfoils for horizontal axis wind turbine blades.

## 2. CFD METHOD OF ANALYSIS

The research's methodology may be quickly explained using a flowchart that lists the many phases needed to complete the study. This flowchart, which is depicted in figure 1, illustrates how all of the methods employed in this research were utilized to analyze and simulate a 2D airfoil.

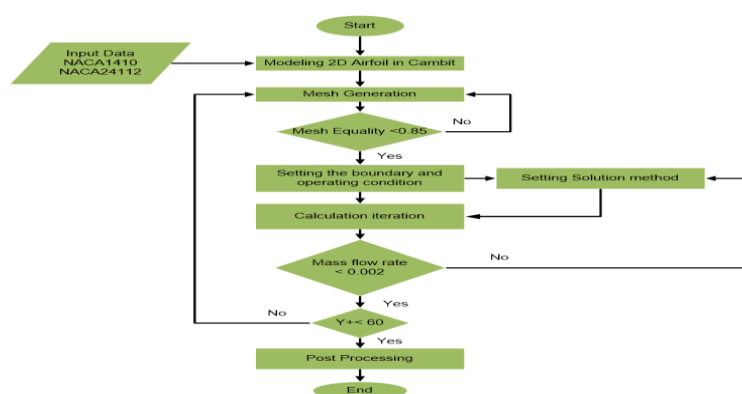


Figure 1. Flowchart of the methodology.

Solidworks produced the NACA 1410 and NACA 24112 airfoils as 2D models as shown in fig2. input coordinates for specific spots made using the Design foil workshop DEMO program.



**Figure 2. NACA airfoils 1410 and 24112**

These airfoils' characteristics start at digit 4, where the maximum camber in chord tenths as measured from LE(40) is located in the same place. However, after designing this airfoil and analyzing its maximum thickness, one was selected for its optimum performance.

These airfoils' characteristics start at digit 4, where the maximum camber in chord tenths as measured from LE(40) is located in the same place. However, after designing this airfoil and analyzing its maximum thickness, one was selected for its optimum performance.

Hexahedral mesh was the sort of material employed in this study, as seen in Figure 3. This mesh's skewness equality score was under 0.85. There are 12270 mesh components in all. The k- turbulence model in Fluent was used to simulate a 2D airfoil for this study. The full set of computational parameters utilized in this simulation are listed in Table 1.

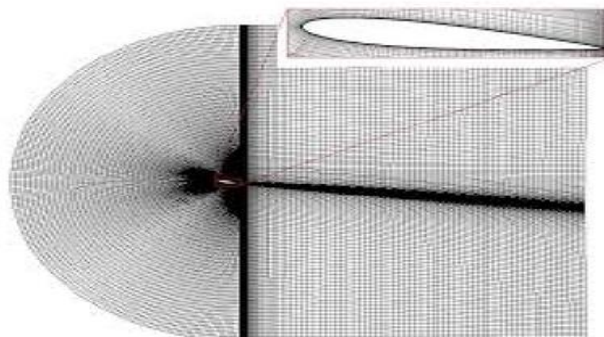


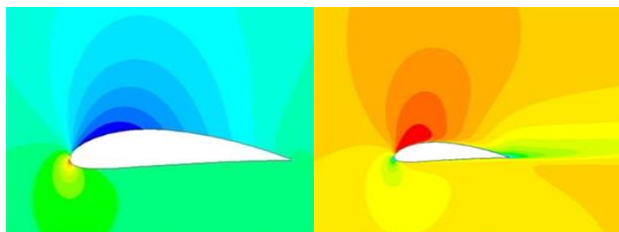
**Figure 3. Topology of computational mesh**

**Table1.** Computational conditions of 2D-dimensional simulation.

NO.	Solver	Pressure based steady
1.	Fluid Material	Air
2.	Density (kg/m <sup>3</sup> )	1.225
3.	Viscosity (kg/m-s)	1.7894
4.	Pressure	101325 pa
5.	Inlet velocity	10 m/s
6.	Pressure couplg	SIMPLE
7.	Momentum	Second order upwind
8.	Boundary	Velocity inlet, pressure

### 3. CONCLUSION AND RESULTS

The NACA 1410 airfoil's pressure and velocity magnitude contours are depicted in Figures 4 through 8. There is an area of high pressure at the leading edge (a point of stagnation) and a zone of low pressure on the top surface of the airfoil. These Figures show that while velocity is higher in the top region and lower in the lower zone, respectively.

**Figure 4.** pressure and velocity plot- 0° Angle of attack**Figure 5.**pressure and velocity plot 7° Angle of attack

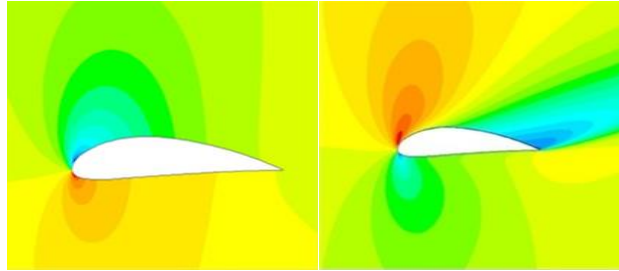


**Figure 6.** pressure and velocity plot- 14° Angle of attack.

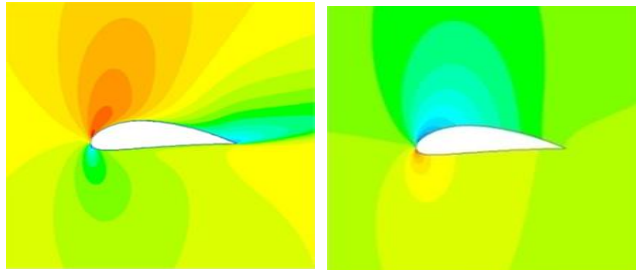


**Figure 7.** pressure and velocity plot- 30° Angle of attack.

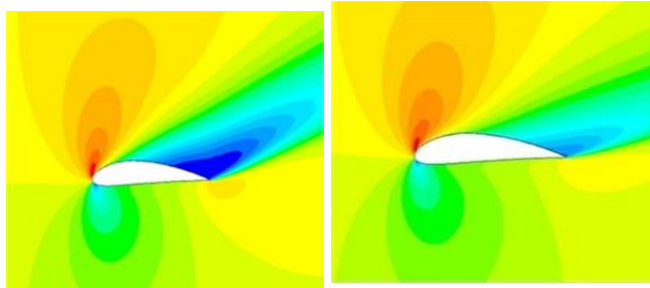


**Figure 8** illustrates pressure and velocity plot- 50° of attack

For a variety of attack angles, the  $C_L$  and  $C_D$  values were discovered. Calculations for the Lift and Drag forces are made for angles of attack of 0, 7, 14, 30, and 50 degrees. For a 10 m/s constant velocity. Table 2 displays the lift, drag, and momentum for various angles of attack.

Table 2. Shows lift and drag and momentum coefficient of NACA1410 for various angles of attack

AOA	CL	Cd	Cm
0	0.5113	0.058368	0.2165
7	0.94674	0.090449	0.32350
14	1.2005	0.1499	0.39120
30	1.3738	0.23650	0.44291
50	1.3672	0.33924	0.44025

The NACA 24112 airfoil's pressure and velocity contours are depicted in Figures 9 through 13. The airfoil has an area of high pressure at the leading edge (also known as a stagnation point) and a zone of low pressure on its top surface. These figures show that the velocity has a smaller magnitude at the bottom and a higher magnitude in the top section.

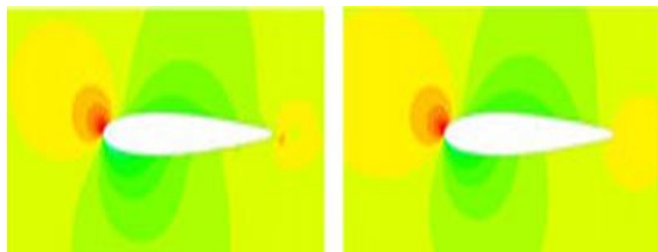


Figure 9. pressure and velocity plot- 0° angle of attack

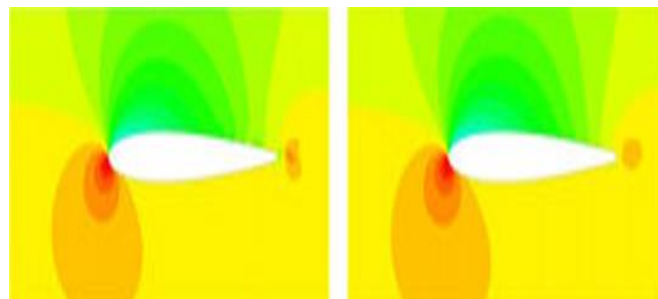
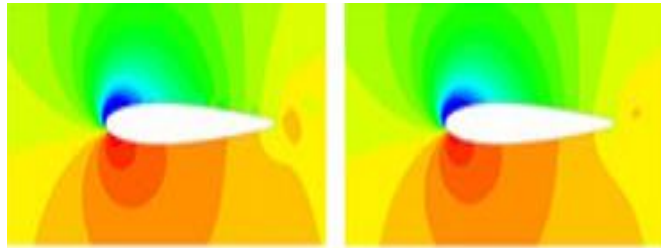
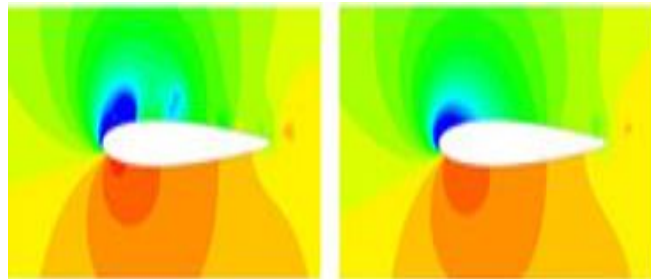


Figure 10. pressure and velocity plot – 7° angle of attack



**Figure 11.** pressure and velocity plot – 14° angle of attack



**Figure 12.**pressure and velocity plot– 30° angle of attack

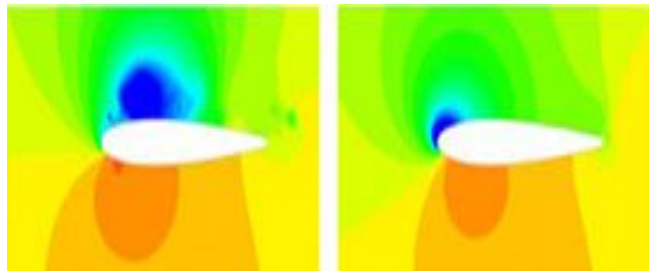


**Figure 13.** pressure and velocity plot– 50° angle of attack.

For a variety of attack angles, the CL and Cd values were discovered. The lift and drag forces are estimated using the (0, 7, 14, 30, 50) degree angle of attack. for the 5 m/sec velocity constant. Table 3 displays the lift, drag, and momentum for various angles of attack

**Table 3.** Shows lift and drag and momentum coefficient of NACA24112 for various angles of attack

OA	CL	Cd	Cm
0	0.3917	0.0764	0.2006
7	0.8089	0.0963	0.2987
14	1.1510	0.1481	0.3746
30	1.3576	0.2243	0.4159
50	1.3930	0.3152	0.4250

Lift coefficient increases until the critical angle of attack is reached. Both the NACA 1410 and the NACA 24112 airfoils have 14° critical angles of attack. NACA1410 airfoil always has a greater lift coefficient and a lower drag coefficient than NACA24112-, as seen in Figure 14.

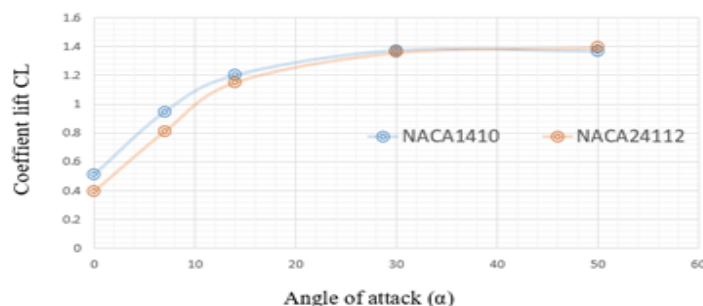


**Figure 14.** Numerical lift and angle of attack curve in comparison with airfoils wind turbine

In Figure 15, the CA24112 airfoil is shown to have a greater lift and drag coefficient ratio under the same AoA as the NACA1410 airfoil. at this NACA 1410 series, the coefficient of lift and drag is determined at angles of attack ranging from 0° to 50°. When the angle is increased, the coefficient of lif rises.

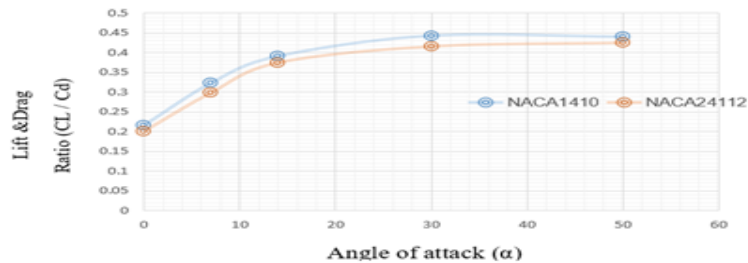


**Figure 15** shows the numerical lift, drag ratio, and angle of attack curve in relation to the wind turbine's airfoil.

#### 4. Conclusions:

This study demonstrated how the 4-digit symmetric airfoils NACA 1410 and NACA 24112 behaved at varied attack angles. The k-epsilon turbulent viscosity model was the best suitable turbulence model for these simulations. For this NA-CA 1410, NACA 24112 series, the coefficient of lift and drag is determined for angles of attack ranging from 0° to 50°. With an increase in angle of attack, the lift/drag ratio coefficient rises by up to 14°. After 14°, the Lift/ Drag ratio falls as the Angle of attack rises. When the angle of attack is between 0° and 50°, the airfoil's upper and lower surfaces are examined for the coefficient of pressure.. According to the findings, the lower surface has a smaller negative coefficient of pressure at a lower angle of attack than the top surface does at a greater angle of attack. From different angles of attack, the lift and drag coefficient curves are displayed and calculated for this study.

---

**REFERENCES**

- [1] National Advisory Committee for Aeronautics, "NACA Report No. 824 – Summary of Airfoil Data", H. Abbott, 2010.
- [2] Second Edition Copyright, Earth scan, UK and USA 8–12 Camden High Street London, O. L. Hansen, "Aerodynamics of Wind Turbines," 2008.
- [3] Science, University of Malaysia.37(2001)365–380. B. Basuno and Z. Abdullah (2001), "Computational aerodynamic analysis of multicomponent airfoil using viscous-in viscid interaction scheme."
- [4] 4th ASME\_JSME Joint Fluids Engineering Conference, Honolulu, Hawaii, USA, July 6–11. O. Badran and H. Bruun, "Turbulent flow over a NACA 1410 airfoil at angle of attack 15 degree," Proceedings of FEDSM'03.
- [5] D. Adair, Experiments in Fluids 5, 114–128 (1987), "Characteristics of a Trailing Flap Flow with Small Separation."
- [6] D. Coles, A. Wadcock, (1979), Flying-hot-wire study of flow past an NACA 1410 airfoil at maximum lift. AIAA 17:4, 321–329.